Earth and Planetary Science Letters, 31 (1976) 239–246

[6]

ON THE APPLICABILITY OF A UNIVERSAL ELASTIC TRENCH PROFILE

J.G. CALDWELL, W.F. HAXBY, D.E. KARIG and D.L. TURCOTTE

Department of Geological Sciences, Cornell University, Ithaca, N.Y. (USA)

Received October 23, 1975
Revised version received March 31, 1976

Using thin elastic plate theory and neglecting horizontal applied forces, a universal deflection profile applicable to many oceanic trenches is derived. This theoretical profile is compared with bathymetric profiles from the central Aleutian, Kuril, Bonin, and Mariana trench–outer rise regions. The profiles were corrected for sediment thickness and age variation of the lithosphere. Good agreement between theory and observation is found. The distance from the first point of zero deflection seaward of the trench to the point of maximum height of the outer rise is directly related to the flexural rigidity of the lithosphere. The thickness of the elastic lithosphere is found to vary between 20 and 29 km for the trench profiles considered. The good agreement obtained shows that horizontal forces may be neglected and that the bending lithosphere behaves elastically in the cases considered. The analysis shows that only unreasonably large horizontal forces would affect the universal deflection curve. It is concluded that although the near-surface lithosphere may be subject to brittle fracture, the deeper lithosphere is capable of transmitting elastic stresses as high as 9 kbar.

1. Introduction

One well-known feature of island arc–trench systems is the outer rise or topographic high which occurs on the order of 100 km seaward of most trench axes. The existence of an outer rise in association with an oceanic trench has been explained in terms of the flexure of an elastic lithosphere acted upon by horizontal and vertical forces [1,2].

Several authors have used thin elastic plate theory to describe the flexure of the lithosphere in the vicinity of oceanic trenches. Gunn [3] used this theory to relate trenches, mountain belts, and volcanic chains. Jeffreys [4] and Heiskanen and Vening Meinesz [5] solved the problem of flexure of an elastic lithosphere for various types of loading. Lliboutry [6] has discussed the mechanism for the underthrusting of the lithosphere at trenches. Walcott [7] has used this type of analysis to determine the flexural rigidity of the lithosphere in different tectonic provinces.

Hanks [1] considered in detail the Kuril trench–Hokkaido rise and concluded that a horizontal compressive stress of several kilobars is required to explain the observed topography. He discussed the role of an applied bending moment but did not include it in his analysis. Le Pichon et al. [8] have given a complete analytic treatment of the problem, including the applied bending moment. Watts and Talwani [2] studied the correlation between gravity anomalies and trench topography. They concluded that they could produce the topography near the southern Bonin and Mariana trenches with zero horizontal force acting on the Pacific plate, but that a horizontal compressive stress of a few kilobars would be required to produce profiles matching those of the eastern Aleutian, Kuril, northern Bonin, Ryukyu, and Philippine trenches. Dubois et al. [9] considered the recent uplift of islands on the outer rise in the New Caledonia–Loyalty Islands area.

In this paper we shall use thin elastic plate theory to produce deflection curves that will be compared in detail to topographic profiles across the central Aleutian, Kuril, northern Bonin, and Mariana trenches. We shall show that these trench profiles can be described by a universal deflection curve and that no horizontal force is required [8,10]. It is also concluded that the lithosphere behaves elastically to the trench axis.

2. The mechanics of lithospheric deformation

In this section we examine the one-dimensional, linear deformation of a thin elastic plate subjected to a hydrostatic restoring force. In the following section, we will compare the theoretical deflection curves with the actual bathymetric profiles of trench–outer rise systems. The differential equation which describes the one-dimensional bending of a thin plate is:

$$D\frac{d^4w}{dx^4} + S\frac{d^2w}{dx^2} + kw = 0 \qquad (1)$$

where w is the vertical deflection of the plate from its equilibrium depth, x is the horizontal coordinate, S is the horizontal loading force (positive for compression), and k is the hydrostatic restoring force per unit deflection, $k = (\rho_m - \rho_w)g$ where ρ_m and ρ_w are the densities of the underlying mantle and overlying water, respectively, and g is the acceleration of gravity. The flexural rigidity of the plate is given by:

$$D = \frac{Eh^3}{12(1-\nu^2)}$$

where E is Young's modulus, h is the thickness of the plate, and ν is Poisson's ratio.

In order to obtain a physically reasonable solution to (1), the vertical deflection of the plate as $x \to \infty$ must approach zero. It is convenient to chose the origin, $x = 0$, as the point nearest the trench axis where the deflection, w, is zero (Fig. 2).

The solution to (1) can now be written:

$$w = A \sin\left[\frac{x}{\alpha}(1+\epsilon)^{\frac{1}{2}}\right] \exp\left[-\frac{x}{\alpha}(1-\epsilon)^{\frac{1}{2}}\right] \qquad (2)$$

where $\alpha^4 = 4D/k$, $\epsilon = S/2(kD)^{\frac{1}{2}}$, and A is a constant to be determined. The constant α is termed the flexural parameter and is a characteristic length for the bending of the plate; ϵ is a dimensionless parameter directly proportional to the horizontal applied force S. If ϵ is greater than one, a solution does not exist; $\epsilon = 1$ corresponds to the first buckling mode of failure [11].

The outer rise of a trench system (Fig. 1) contains the point of maximum positive deflection, whose magnitude and coordinate are denoted by w_b and x_b respectively (Fig. 2). The values of w_b and x_b may be obtained from corrected bathymetric profiles. The following equations give x_b and w_b in terms of the constants

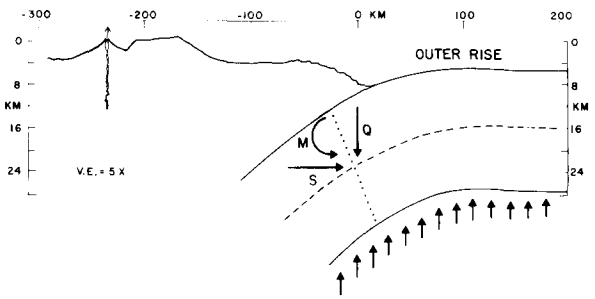

Fig. 1. A schematic cross-section of an island arc system showing the relative position and amplitude of the outer rise. The descending lithosphere is about 25 km thick, corresponding to its effective elastic thickness. The three arrows converging at the dotted line indicate that any arbitrary section through the lithosphere is acted upon by a vertical shear force Q, a horizontal force S, and a bending moment M.

α and ϵ:

$$x_b = \frac{\alpha}{(1+\epsilon)^{\frac{1}{2}}} \arctan\left(\frac{1+\epsilon}{1-\epsilon}\right)^{\frac{1}{2}} \qquad (3)$$

$$w_b = \frac{A(1+\epsilon)^{\frac{1}{2}}}{2^{\frac{1}{2}}} \exp\left[-\frac{x_b}{\alpha}(1-\epsilon)^{\frac{1}{2}}\right] \qquad (4)$$

We now make the assumption that $\epsilon \ll 1$ and expand (3) and (4) retaining only those terms linear in ϵ with the result:

$$x_b = \frac{\alpha\pi}{4}\left[1 + \left(\frac{4}{\pi} - 1\right)\epsilon\right] \qquad (5)$$

$$w_b = \frac{A}{2^{\frac{1}{2}}} e^{-\pi/4}\left(1 + \frac{\pi}{4}\epsilon\right) \qquad (6)$$

In order to estimate the value of ϵ we set $S = \overline{\sigma_{xx}}\,h$, where $\overline{\sigma_{xx}}$ is the mean horizontal stress across the thickness h of the plate. Then:

$$\epsilon = \overline{\sigma_{xx}}\left(\frac{3(1-\nu^2)}{hkE}\right)^{\frac{1}{2}} \qquad (7)$$

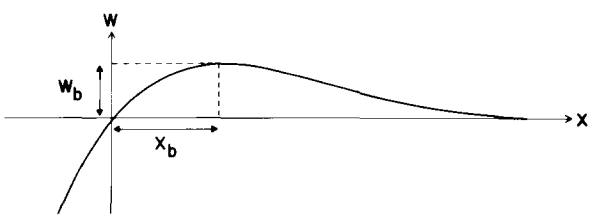

Fig. 2. A plot of a deflection curve defining the quantities w_b and x_b.

Typical values for the constants in this equation are $E = 6.5 \times 10^{11}$ dyne/cm^2; $\nu = 0.25$; $k = 2.4 \times 10^3$ dyne/cm^2; and $h = 25$ km. For an average stress of 10 kbar ϵ is approximately 0.3. The error in determining α from x_b by setting $\epsilon = 0$ in (5) is less than 5%; the corresponding error in determining A from w_b by setting $\epsilon = 0$ is about 25%. It is concluded that even a large horizontal load will not have a strong effect on the deformation of the plate, and that S cannot be determined from bathymetric profiles with any precision.

In the remainder of this paper we will consider the limit $\epsilon = 0$. We will show that there is good agreement between theory and observations in this limit. Setting $\epsilon = 0$ in (5) yields:

$$x_b = \frac{\pi\alpha}{4} = \frac{\pi}{4}\left(\frac{4D}{k}\right)^{\frac{1}{4}} \tag{8}$$

The distance x_b is a direct measure of the flexural rigidity and, therefore, of the thickness of the elastic lithosphere.

Setting $\epsilon = 0$ in (2) gives:

$$w = Ae^{-x/\alpha} \sin x/\alpha \tag{9}$$

We now introduce non-dimensional variables $\bar{x} = x/x_b$, and $\bar{w} = w/w_b$. From (6), (8), (9) we obtain:

$$\bar{w} = 2^{\frac{1}{2}} \sin\left(\frac{\pi\bar{x}}{4}\right)\exp\left[\frac{\pi}{4}(1-\bar{x})\right]$$

This is a universal equation describing the deformation of the oceanic lithosphere at a trench under the assumptions made above. Observations will be compared with this universal trench profile in the next section.

This analysis also gives the bending moment and shearing force at any point on the deformed plate. We introduce the following non-dimensional bending moment $\bar{M}$ and shear force $\bar{Q}$:

$$\bar{M} = Mx_b^2/Dw_b, \qquad \bar{Q} = Qx_b^3/Dw_b$$

where M and Q are the dimensional bending moment and shear force, respectively. Taking derivatives of (9), the dependence of $\bar{M}$ and $\bar{Q}$ on the horizontal coordinate $\bar{x}$ is given by:

$$\bar{M} = \frac{2^{\frac{1}{2}}\pi^2}{8}\cos\left(\frac{\pi\bar{x}}{4}\right)\exp\left[\frac{\pi}{4}(1-\bar{x})\right] \tag{10}$$

$$\bar{Q} = -\frac{2^{\frac{1}{2}}\pi^3}{32}\left[\cos\left(\frac{\pi\bar{x}}{4}\right)+\sin\left(\frac{\pi\bar{x}}{4}\right)\right]\exp\left[\frac{\pi}{4}(1-\bar{x})\right] \tag{11}$$

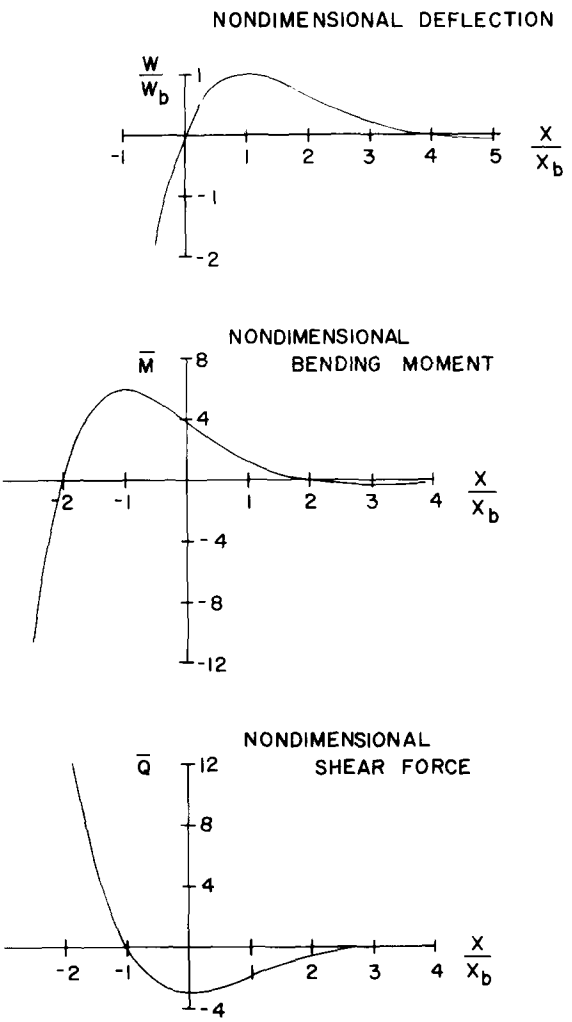

Fig. 3. Graphs of the non-dimensional deflection of a thin elastic plate and the associated non-dimensional bending moment and shear force.

The solutions for $\bar{M}$ and $\bar{Q}$ are plotted, along with the solution for $\bar{w}$, in Fig. 3.

3. Observations

We now compare the universal deflection curve using various values of w_b and x_b with observed topographic profiles across four trench–outer rise systems: the central Aleutian, the Kuril, the Bonin, and the Mariana (Fig. 4). The profiles extend from about the trench axis to roughly 300 km seaward of the axis, include the

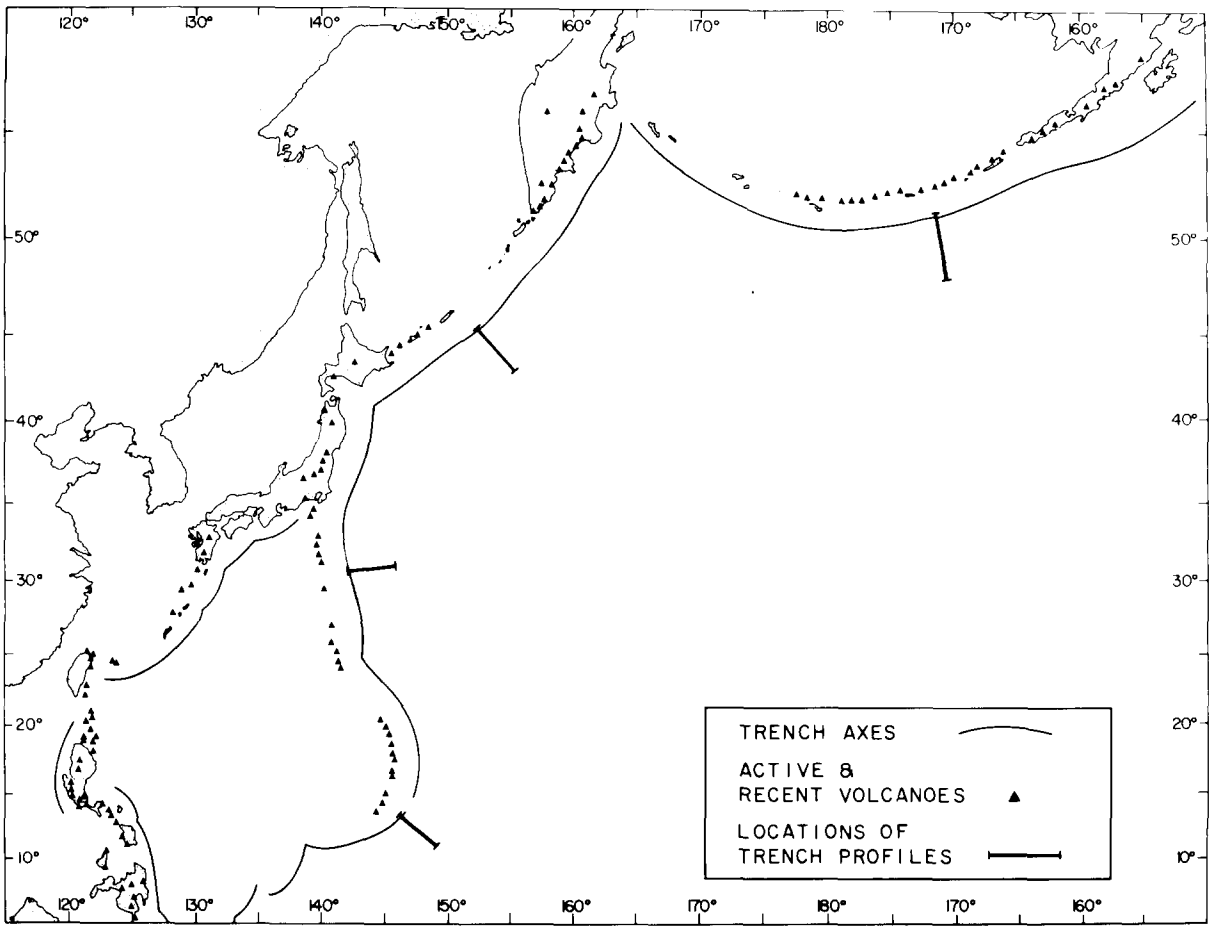

Fig. 4. Map (after Karig and Sharman [16]) showing the locations of the corrected bathymetric profiles.

outer rise, and are projected perpendicular to the particular trench axis. In our analysis several profiles in a region were considered to insure that representative profiles were used. To compare the universal curve with the observed topographic profiles, a base reference line that corresponds to the undeflected ocean floor must be determined. In order to determine this reference line, corrections must be applied to the observed profiles. These corrections arise due to the variations in thickness of the sediment cover on the sea bottom and due to variations in age for different regions of the oceanic lithosphere.

Seismic reflection profiles are used to make the necessary sediment correction. We assume that the deepest reflector on seismic reflection profiles follows the contours of the basement. We used the bathymetric profiles as the data base, since they are more numerous than seismic reflection profiles. Data from corresponding or nearby seismic reflection profiles were used to give the variations in sediment thickness along a given profile. We removed the measured thickness of the sediment cover, taking into account the isostatic unloading effect on the lithosphere. For this calculation we used $\rho_w = 1.0$, $\rho_{sediment} = 1.6$, $\rho_m = 3.4$. For the trench-rise regions we considered, this correction was a substantial portion of the observed topographic amplitude of the outer rise. For the central Aleutian, Kuril, and Bonin outer rises the sediments are much thicker on the rise than they are seaward, so that the correction effectively lowers the maximum height of the rises by 130 m [17], 330 m [18], and 130 m respectively. In contrast, the sediments are thicker seaward of the rise

associated with the Mariana trench, so the correction effectively increases the rise amplitude by 210 m [19].

The other correction which is of importance is that due to the age variation of the lithosphere and the corresponding increase in depth of the ocean floor with increase in age [12]. For the three western Pacific trenches which we matched, the age corrections were ignored because the age of the lithosphere being subducted is greater than 110 m.y. [13]. However, the correction is significant for the profile across the central Aleutian trench—rise with a maximum reduction of the rise amplitude of some 110 m since the age of the ocean floor at the trench is 62.5 m.y. (anomaly 27) and at the seaward end of the profile is 70.5 m.y. (anomaly 32) [14].

Direct measurement of w_b and x_b was often difficult because of local topographic irregularities. Therefore, to obtain the first point of zero deflection on the corrected bathymetric profile, theoretical curves with different w_b and x_b values were fitted to the corrected profile. The best fit determined the point of zero deflection and the best values for w_b and x_b.

Topographic irregularities such as seamounts and vertical offsets made it difficult to fit some profiles. Fig. 5 illustrates this problem by showing five profiles across the Bonin trench; the northernmost profile (E) is separated from the southernmost (A) by only 3.5°. Since it had the least extraneous topography, profile A was used to determine the best fit to the theoretical curve. This best-fitting theoretical curve A is compared with the other profiles in Fig. 6. Despite the presence of seamounts and other topographic features, the profiles are in quite good agreement with the theoretical curve.

The main results of this paper are summarized in Fig. 6. The solid curve is the universal deflection curve

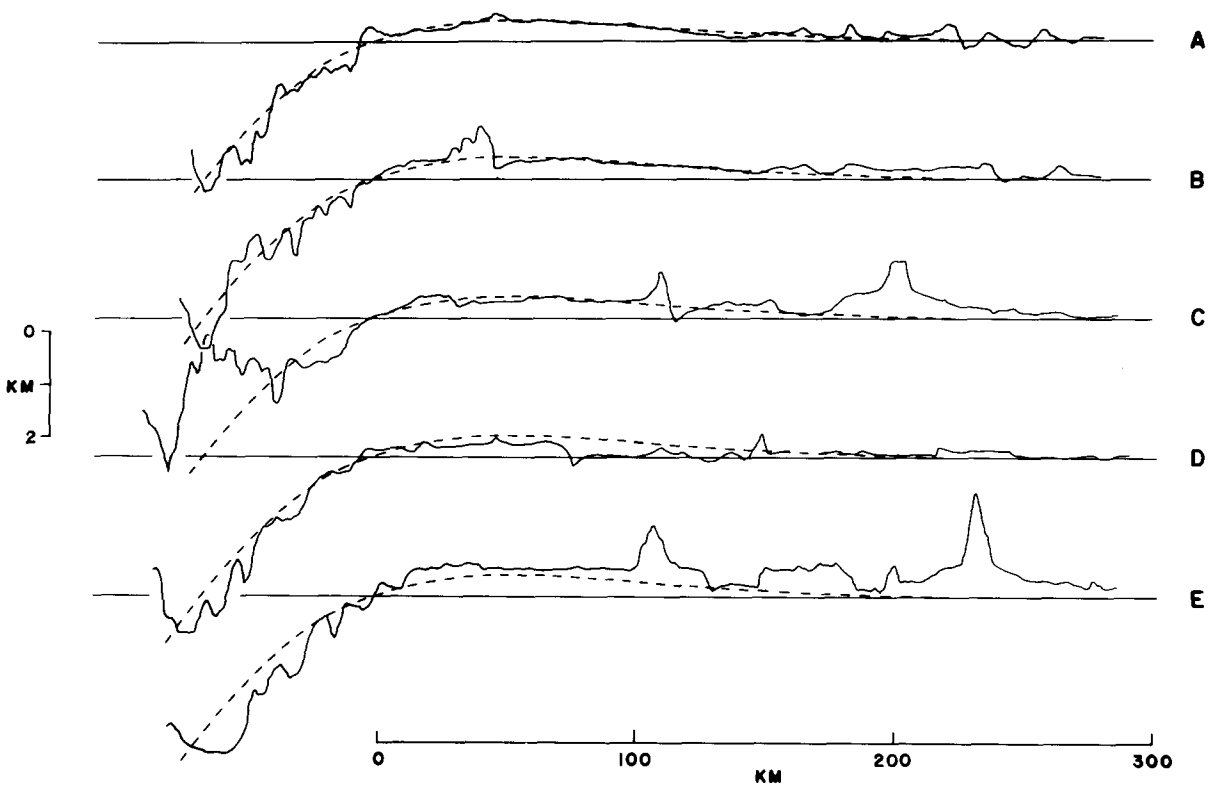

Fig. 5. Five profiles located between 30°30'N and 34°N across the Bonin trench. The dashed line is the best-fitting theoretical curve for profile A and is plotted for comparison with each of the other profiles. Sources of bathymetric data are Hunt 3 (profiles A and C), Aries 7 (profile B), Antipode 3 (profile D), and Japanyon 4 (profile E) cruises, and of seismic reflection data are Antipode 3 and Aries 7 cruises (SIO and NAVOCEANO data published with permission).

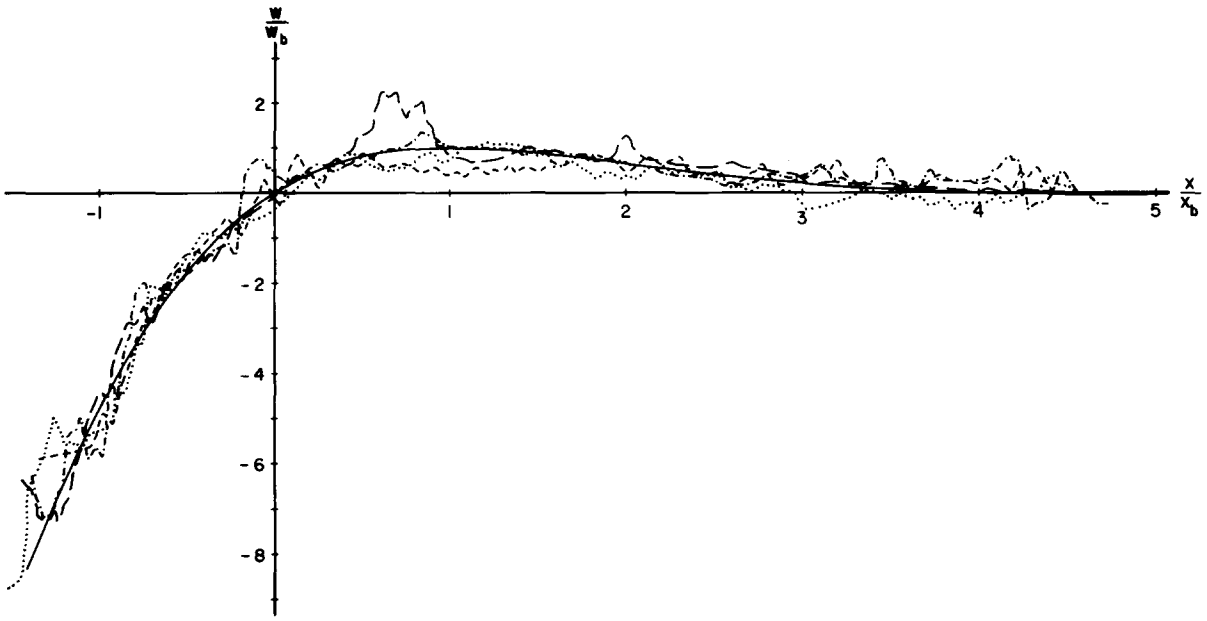

Fig. 6. The solid line is the universal deflection curve and the broken lines are the corrected and normalized bathymetric profiles. – – – is the Mariana profile (data from Scan 5 cruise and [19]), – · – · is the Bonin profile (Hunt 3 and Aries 7 cruises), · · · · · is the Kuril profile (Zetes 2 cruise and [18]), and - - - - - is the central Aleutian profile (Seamap 13 cruise and [17]).

TABLE 1

Trench parameters

Trench name	Mariana	Bonin	Aleutian	Kuril
x_b (km)	55	53	53	42
w_b (km)	0.50	0.40	0.35	0.28
Flexural rigidity (dyne cm)	1.4×10^{30}	1.2×10^{30}	1.2×10^{30}	0.5×10^{30}
Lithospheric thickness (km)	29	28	28	20
Trench axis distance from point of zero deflection (km)	71	70	58	68
Maximum bending stress (kbar)	9.2	7.6	6.6	6.2
Point of maximum bending stress (in km) seaward of trench axis	20	20	8	30
Shear force at trench axis (dyne/cm)	1.0×10^{15}	9.8×10^{14}	3.1×10^{14}	1.4×10^{15}
Bending moment at trench axis (dyne)	1.3×10^{22}	9.5×10^{21}	8.9×10^{21}	2.8×10^{21}
Shear force at point where bending moment equals zero (dyne/cm)	8.0×10^{15}	5.3×10^{15}	4.6×10^{15}	3.2×10^{15}
Point of zero bending moment (in km) landward of trench axis	50	40	50	20

from (10) which describes the flexure of all thin elastic plates acted upon by a vertical force and a bending moment. The broken curves are the various corrected trench profiles that have been normalized by their respective w_b and x_b values.

Table 1 gives the values of x_b and w_b for the best fits. Also given are the corresponding values of the flexural rigidity obtained from x_b using (8) taking $k = 2.4 \times 10^3$ dyne/cm^2. The equivalent thicknesses of the elastic lithosphere are tabulated using the definition of the flexural rigidity and taking $E = 6.5 \times 10^{11}$ dyne/cm^2 and $\nu = 0.25$. The maximum bending stress (the stress on the top edge of the plate at the point of greatest curvature) for each trench is also given. The largest bending stress we find is 9.2 kbar, and occurs 20 km seaward of the Mariana trench axis.

In general the fit of the profiles to the universal curve is quite good; however, the Aleutian profile does lie below the universal curve near the highest part of the rise. This is not a spurious feature of this particular profile since the same deviation occurs on two other nearby profiles.

4. Discussion

The shape and amplitude of the observed profiles from the trench axis through the outer rise region are very similar to those produced by a thin elastic plate when that plate is acted upon by a combination of a vertical force and bending moment. The fact that the fit between the observation and the theory is so close strongly suggests that the lithosphere behaves dominantly elastically even for stresses as high as 9 kbar. Since the bending of the lithosphere is convex, the upper part of the lithosphere is in tension. It is doubtful that the near-surface rocks where the hydrostatic pressure is low can sustain this high a tensional stress. Therefore, near-surface block faulting can be expected. This would explain the observed normal faulting in this region [15]. However, the good agreement between observations and elastic theory precludes fractures of the entire lithosphere or plastic bending in the region of maximum stress seaward of the trench axis.

We have not considered in this paper trenches where very young lithosphere is being subducted, i.e., the Middle America trench, or where marginal basin lithosphere is being subducted, i.e., the New Hebrides trench. In these cases preliminary studies indicate that the height of the outer rise is less than the value predicted from the universal profile and therefore elastic theory may not be applicable.

In achieving the good agreement between the actual profiles and theoretical ones, the condition of zero horizontal force was used in the calculations. If a horizontal force had been incorporated in the analysis, no discernable difference would have occurred unless the magnitude of the stress had been greater than about 10 kbar. While this study has shown that no horizontal force is required to produce deflections that match observed profiles, horizontal forces may be acting on the descending plate, but pieces of data other than bathymetric data are needed, such data as focal mechanisms of hypocenters seaward of the trench axis which Hanks [1] utilized.

The difference found between the x_b values of the Kuril trench and the other trenches is large enough to suggest that there may be a significant difference in their flexural rigidities. However, there is no obvious explanation for the difference. The age of the lithosphere is roughly the same for the Mariana, Bonin, and Kuril areas, and if a difference in age should show up as a difference in flexural rigidity, the central Aleutian trench should have the lowest flexural rigidity. It is possible that horizontal forces alter the effective elastic thickness, hence the flexural rigidity, of the lithosphere. The effective thickness is the region where elastic behavior occurs. In bending a plate, the upper part is placed in tension, the lower part in compression. The lower part will become plastic when the compressive stress reaches some limit. A compressive horizontal force will reduce the amount of bending necessary to attain this limit. A similar argument could be made regarding tensional stresses. It is possible that a large horizontal force could explain why the elastic part of the plate in the Kuril region is so thin.

Acknowledgements

This study was supported by NSF grant DES 75-0415. We would like to thank the Scripps Institution of Oceanography and in particular George F. Sharman for supplying many of the profiles used in this paper.

Cornell University Department of Geological Sciences Contribution No. 568.

References

1 T.C. Hanks, The Kuril trench–Hokkaido rise system: large shallow earthquakes and simple models of deformation, Geophys. J.R. Astron. Soc. 23 (1971) 173.

2 A.B. Watts and M. Talwani, Gravity anomalies seaward of deep-sea trenches and their tectonic implications, Geophys. J.R. Astron. Soc. 36 (1974) 57.

3 R. Gunn, Quantitative aspects of juxtaposed ocean deeps, mountain chains and volcanic ranges, Geophysics 12 (1947) 238.

4 H. Jeffreys, The Earth (Cambridge University Press, Cambridge, 1970) 525 pp.

5 W.A. Heiskanen and F.A. Vening Meinesz, The Earth and its Gravity Field (McGraw-Hill, New York, N.Y., 1958) 470 pp.

6 L. Lliboutry, Sea-floor spreading, continental drift and lithosphere sinking with an asthenosphere at melting point, J. Geophys. Res. 74 (1969) 6525.

7 R.I. Walcott, Flexural rigidity, thickness, and viscosity of the lithosphere, J. Geophys. Res. 75 (1970) 3941.

8 X. Le Pichon, J. Francheteau and J. Bonnin, Plate Tectonics (Elsevier, Amsterdam, 1973) 300 pp.

9 J. Dubois, J. Launay and J. Recy, Uplift movements in New Caledonia–Loyalty Islands area and their plate tectonics interpretation, Tectonophysics 24 (1974) 133.

10 B. Parsons and P. Molnar, The origin of outer topographic rises associated with trenches (1975) in press.

11 S. Goldstein, The stability of a strut under thrust when buckling is resisted by a force proportional to the displacement, Proc. Cam. Philos. Soc. 23 (1926) 120.

12 J.G. Sclater, R.N. Anderson and M.L. Bell, Elevation of ridges and evolution of the central eastern Pacific, J. Geophys. Res. 76 (1971) 7888.

13 R.L. Larson and T.W.C. Hilde, A revised time scale of magnetic reversals for the early Cretaceous and late Jurassic, J. Geophys. Res. 80 (1975) 2586.

14 J.G. Sclater, R.D. Jarrard, B. McGowran and S. Gartner, Jr., Comparison of the magnetic and biostratigraphic time scales since the late Cretaceous, in: Initial Reports of the Deep-Sea Drilling Project 22 (U.S. Government Printing Office, Washington, D.C., 1974) 381.

15 W.J. Ludwig et al., Sediments and structure of the Japan trench, J. Geophys. Res. 71 (1966) 2121.

16 D.E. Karig and G.F. Sharman, Subduction and accretion in trenches, Bull. Geol. Soc. Am. 86 (1975) 377.

17 D.E. Hayes and M. Ewing, Pacific boundary structure, in: The Sea, 4, A.E. Maxwell, ed. (Wiley-Interscience, New York, N.Y., 1968) 29.

18 W. Wertenbaker, The Floor of the Sea (Little, Brown and Company, Boston, Mass., 1974) 275 pp.

19 D.E. Karig, Site surveys in the Mariana area (Scan IV), in: Initial Reports of the Deep-Sea Drilling Project 6 (U.S. Government Printing Office, Washington, D.C., 1971) 681.